A PROJECT REPORT
ON

A Study on the Synthesis of Bi-metallic copper-silver nanoparticle & its anti-bacterial potency against multi-drug resistant diarrhea-causing *E.coli* ETEC in vitro and in vivo in mice

Under the guidance of

Dr.Tarak Das Basu

Professor of Biophysics

Department of Biophysics and Biochemistry, University of Kalyani

Submitted by

SUBHAJIT KUNDU

REGISTRATION NO : - 142842 of 2017-18

ROLL NO : - 001720501023

In partial fulfilment for the of the degree

of

MASTER OF SCIENCE

IN

"LIFE SCIENCE AND BIOTECHNOLOGY"

DEPARTMENT OF LIFE SCIENCE AND BIOTECHNOLOGY

JADAVPUR UNIVERSITY

188, Raja S.C. Mallick Road,

Kolkata - 700032

INDEX

ABBREVIATIONS

- NPs : Nanoparticles
- ETEC : Enterotoxigenic Bacteria
- PVP : Poly-Vinyl Pyrrolidone
- DLS : Dynamic light scattering
- AFM : Atomic force microscopy
- Cu@Ag : Copper and silver
- PDI : Polydispersity Index
- NB : Nutrient broth
- Tet^r : Tetracycline resistance
- SB : Starvation Buffer
- NA : Nutrient agar
- MIC : Minimum Inhibitory concentration
- MBC : Minimum Bacterial concentration
- DAI : Disease activity Index
- SPR : Surface Plasmon resonance
- D_H : Hydrodynamic diameter
- LPS : Lipopolysaccharide
- Wt. : Weight
- UV-Vis : Ultraviolet – visible
- MDR : Multi drug resistance

ACKNOWLEDGMENT

The success and final outcome of this project required a lot of guidance and assistance from many people. The internship opportunity I had in **Kalyani University** under the guidance of **Dr. Tarak Das Basu,** department of **Biophysics and Biochemistry, Kalyani University** and under the supervision of my research scholar Mr. **Biplab Chatterjee** was a great chance for learning and professional development. Therefore, I consider myself as a very lucky individual as I was provided with an opportunity to be a part of it. I am also grateful for having a chance to meet so many wonderful people and professionals who led me through this internship period.

I owe my deep gratitude to my project guide **Dr. Tarak Das Basu,** who took keen interest on my project and guided me all along, till the completion of the project work by providing all the necessary information for developing a good system.

I also owe my deep gratitude and thanks towards my volunteer research scholar **Biplab Chatterjee** who devoted their time and knowledge in the implementation of this project.

I heartly thanks to my H.O.D **Prof. Biswadip Das** department of **Life science & biotechnology, Jadavpur University** for suggesting me to do my internship over there.

Nevertheless, I express my gratitude toward my **family members** and **colleagues** for their kind co-operation and encouragement which help me in completion of this project.

Finally, I would like to thank **God** almighty for giving me the strength, knowledge, ability and opportunity to undertake this research study and to persevere and complete it satisfactorily.

Sincerely,

NAME -

PLACE -

DATE -

ABSTRACT

The development of easy methods of preparation metallic nanoparticles (NP) has been very much attracting to the field of material science, from their application potential in different areas, due to their unusual size-dependent optical and electronic properties. This study deals with the development of a simple robust method of synthesis of simple bimetallic copper-silver nanoparticles (Cu-AgNP) by successive reduction of Cu $(No_3)_2$

and $AgNo_3$, using **hydrazine hydride** as the reducing agent and **gelatine** and **poly-vinyl pyrrolidone** (PVP) as the capping agents (stabilizer). The round shaped particles were of core-shell structure with a core of Cu^0 atoms surrounded by a shell of Ag^0 atoms. The **size** and **Zeta potential** of the NPs were (76.26) nm and (-15.5) mV respectively. The particles were crystalline in nature and 90% of the precursors $Cu(No_3)_2$and $AgNo_3$ were converted to Cu-Ag NPs. The NPs were characterized by the techniques like **dynamic light scattering** (DLS), **atomic force microscopy** (AFM) etc.

The NPs were toxic to multi-drug (cefixime, ceftriaxone, erythromycin, sulfamthoxazole, trimetthoprin, vancomycin, tetracycline, rifaximin etc.) resistant **Enterotoxigenic Bacteria** (ETEC) that killed most of the ETEC. Therefore, Cu-Ag NPs can be used as a potent antibacterial drug in future. The antibacterial activity of this Cu-Ag NPs on Gram negative ETEC was demonstrated by agar plating method. Determination of the **minimum inhibitory concentration** (5.483µg/ml), **minimum bacterial concentration** (6.27µg/ml), showed that our Cu-Ag NPs were highly effective at lower concentration than that of any antibiotic.

INTRODUCTION

Nanotechnology is a new area in the field of science that works with materials at nanoscale level and blurs the boundary between Physics, Chemistry and Biology. The elimination of these boundaries poses a new direction to the **organization of education and research.** The nanometer world is a particular domain where the dimensions and different physio-chemical characteristics of materials undergo drastic changes from those of their bulk form.

Richard Feynman a famous physician 1st gave the idea of Nano-world in his famous talk on "There's plenty of room at the bottom". The term nanotechnology was first defined by the Tokyo Science University Professor **Norio Taniguchi** in 1974 in a paper entitled "Nanotechnology mainly consists of processing of seperation, deformation and consolidation of material by one atom or one molecule".

Nanoparticles are defined as very tiny particles whose dimension is of the order of a millionth of a meter.

The project focuses on the synthesis and use of nanoparticles in biology. Diarrheal disease caused by principal bacterial genii *Escherichia*, *Salmonella*, *Shigella* etc. represents a major health problem in developing countries where death occurs in children upto 5 years of age. This is due to unresponsiveness of microbes to diverse classes of drugs with different mechanisms of cytotoxic action, generally referred to as Multi Drug Resistance (MDR).One of the multi-Drug resistant *E.coli* is ***Enterotoxigenic*** **ETEC,** that is resistance to a wide varieties of antibiotics (cefixime, ceftriaxone, erythromycin, sulfamthoxazole, trimetthoprin, vancomycin, tetracycline, rifaximin etc.). The annual death due to multidrug resistant *Staphylococcusaureus* (MRSA) infection has increased from 1lakh to 3lakhs. A Bacteria survives due to different kinds of adaptations like **mutation, efflux, enzymatic clearanceofdrugs, conjugation, transformation** etc. Nanoparticles due to their small size are more effective than its bulk form due to the presence of its large surface area to volume ratio.

$$\frac{\text{Surface Area}}{Volume} \alpha \frac{1}{r}$$

i.e. smaller the radii of the particles, greater the surface area for it to cause challenge in the bacterial membrane permeability. The accumulation of NPs or their ions within bacterial cells generates ROS and subsequently causes oxidative damage to the cell structure, followed by depletion of intracellular ATP production and disruption of DNA replication. Low molecular wt. of NPs kills/inhibits broad spectrum pathogenic bacteria. The most promising NPs are metallic but bimetallic NPs may enhance the properties further. The reason behind why Cu@Ag NPs has been chosen in this regard is,

1. Its high antibacterial property
2. High Electron conductivity
3. Lower toxicity to humans
4. Possess different chemical, physical, magnetic, optical, catalytic properties
5. Lead free solder alloy.

In this communication, we will report about:-

I. A simple, economic and chemical reduction method of synthesis of stable Cu@Ag NPs suspension.
II. Characterization of optical properties, size, shape, Zeta potential, molecular wt., and composition of NPs.
III. Determination of antibacterial properties (MIC & MBC) of the NPs and their subsequent ions.
IV. The occurrence of cell filamentation due to inhibition of cell division was the type of cell damage incurred by the bacteria.

V. V. In vivo analysis of the effect of NPs and subsequent ions on ETEC-infected Balb/C Mice, suffered from diarrhea.

METHODOLOGY

1. ETEC

Diarrheagenic *E.coli* belongs to different categories based on their virulence, mechanism, epidemiology, and serotypes. Currently five distinct categories of Diarrheagenic *E.coli* are recognised:-

Enteropathogenic *E.coli* (EPEC),**Enterotoxigenic *E.coli*** (ETEC), **Enteroinvasive *E.coli*** (EIEC), **Enterohemorrhagic *E.coli*** (EHEC), **Enteroaggregative *E.coli*** (EAEC). ETEC is a type of *E.coli* which is one of the leading bacteria that causes diarrhoea in the developing countries as well as the most common cause of traveller's diarrhoea. These strains produce both **heat liable enterotoxin** (LT) or **heat stable entertoxin** (ST) or both. This is not sufficient for ETEC to cause diarrhoea. The organism must adhere to the mucosal surface of the epithelial cells of the small intestine. This process is mediated by **fimbriae** (**Colonization factors**) which bind to the specific receptors in the cell membrane. LT are protein complexes consists of one polypeptide A subunit and five polypeptide B subunits with molecular weights of 25000 and 11500 respectively. The B subunit is responsible for binding of the toxin to the epithelial cells. After translocation across the membrane of intestinal epithelial cells (NAD)-dependent activation of adenylatecyclase to cause an increase in concentration of cAMP. In the intestinal villus cells, cAMP inhibits the absorption of sodium and therefore chloride and water while in the crypt cells cAMP increases sodium secretion and causes loss of chloride and water, leading to profuse diarrhoea.

2. DLS

Dynamic light scattering (also known as PCS - Photon Correlation Spectroscopy) is a useful technique for the determination of size distribution profile of smaller particles. In this zetasizer instrument, a laser beam (for Zetasizer 633nm) strikes the sample for illumination and the fluctuations of the scattering light are collected at a known scattering angle ø by a fast photon detector. Particles can be spread widely in a variety of liquids. Only liquid refractive Index and viscosity have to be known for interrupting the measurement results. The gained optical signal represents random changes due to the randomly changing relative position of the particles. The "noise" also known as "**Brownian motion**" is in fact due to the particle motion and random collision with the molecules of the liquid that surrounds the particle. An important feature of Brownian motion for DLS is that small particles move quickly and large particles moves slowly. The relationship between the size (**hydrodynamic size**) of a particle and its speed due to Brownian motion is defined by Stokes-Einstein equation-

$$\mathbf{D}_{\mathrm{H}} = \frac{kT}{f} = \frac{kT}{3\pi\eta D}$$

Where $\mathbf{D_H}$: Hydrodynamic diameter, **k**: Boltzmann Constant, **f**: particle frictional constant, **η**: solvent viscosity, **T**: Absolute temperature, **D**: Diffusion Coefficient. As the particles are constantly in motion the speckle pattern will also appear to move. As the particle move around, the constructive and destructive phase addition of the scattered light will cause the bright and dark areas to grow and diminish/fluctuate in intensity. The Zetasizer Nano system measures the rate of intensity fluctuation and then uses this to calculate the size of the nanoparticle.

2.1. **Zeta Potential-** It is the potential difference between the dispersion medium and the stationary layer of fluid attached to the dispersed particles. It is caused by the net electrical charge contained within the region bounded by the slipping plane and also on the location of that plane.

Ions close to the surface of the particle will be strongly bound and hence named **Stern Layer** while ions that are further away will be loosely bound forming what called **Diffuse Layer**. Within the diffused layer there is a notional boundary is called **SlippingPlane .**It is a key indicator of the stability of colloidal dispersion .The magnitude of Zeta potential indicates the degree of electrostatic repulsion between adjacent, similarly charge particles in dispersion. For molecules and particles that are small enough, high Zeta potential will confer stability i.e. the solution will resist aggregation. When the potential is small, attractive forces may overcomes this repulsion force and the solution may break and flocculate and nanoparticles aggregate and precipitate down as outline in the table below.

Zeta Potential{mV}	**Stability behaviour of NPs**
From 0 to ±5	Rapid coagulation or flocculation
From 10 to ± 30	Incipient stability
From 30 to ± 40	Moderate stability
From 40 to ± 60	Good stability
Above ± 60	Excellent stability

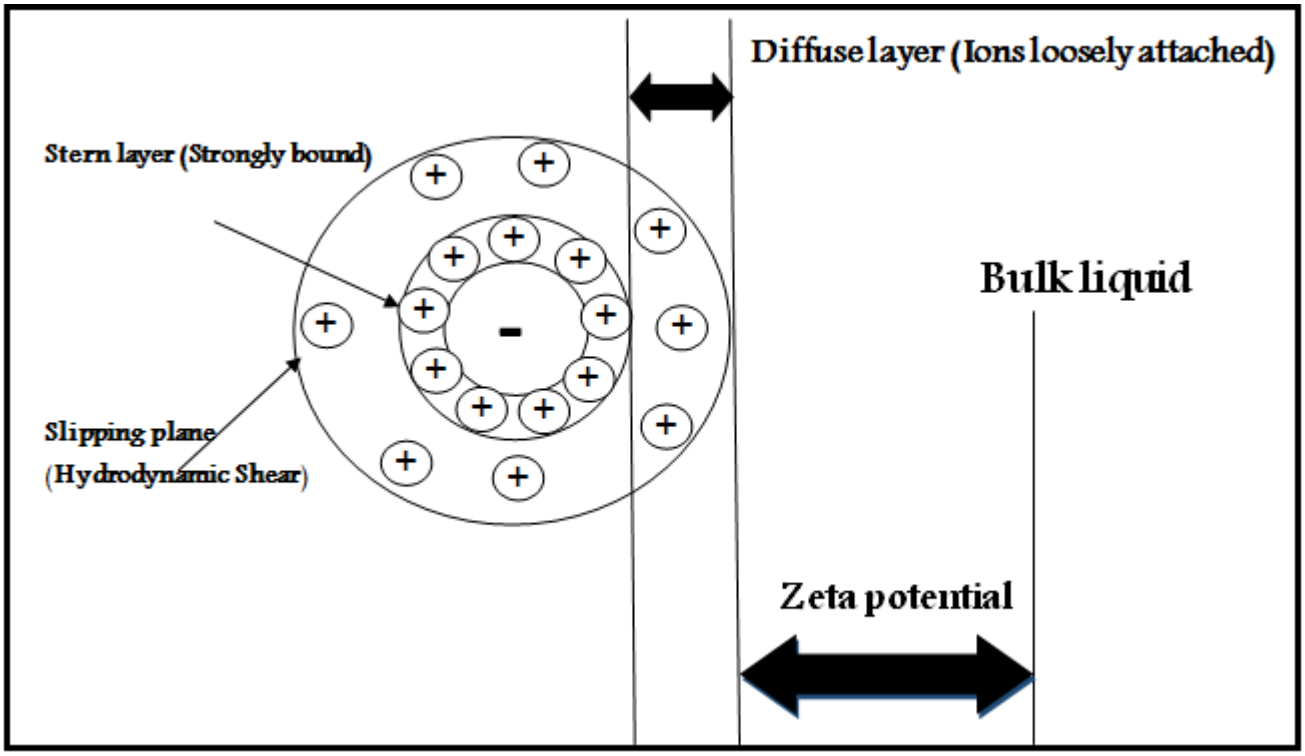

2.2. **Poly Dispersity Index -** It is measure of the distribution of molecular mass of a given sample to measure whether the particles are purely homogenous, intermediate or totally heterogeneous in size. A mono-dispersive sample means that the sample has uniform size distribution; on the other hand, a poly-dispersive sample means that the sample contains non- uniform size range.

$$\text{PDI} = \frac{\text{Square of standard deviation}}{\text{Mean diameter}}$$

PDI value generally ranges from 0-1. If the PDI value falls in the range of 0-0.08, the sample is nearly monodispersive in nature, if the range is in between 0.08-0.7 then the sample is slightly polydispersive (heterozygous range), finally if the range is in between 0.7-1, the sample is highly polydispersive i.e. the sample has a very broad distribution of particle size.

3. Fluorescence Microscopy

Fluorescence is the emission of light that occurs within nanoseconds after absorbing light that is typically of shorter wavelength. The difference between the exciting and emitted wavelengths known as Stokes Shift, is the critical property that makes fluorescence so powerful. The preferred approach in modern fluorescence is epi-illumination. The excitation of flurophore is equivalent in both epi and transmitted microscopes, only a small percentage of the exciting light that is reflected off the sample

needs to be blocked in the return light path in the epi-illumination mode. The main technical problem with this approach is that the exciting light and fluorescence emission overlap in the light path requiring a special kind of beam splitter, a **dichroic mirror** placed at an angle of **45**°, to separate the excitation from the emission.Since most of the excitation light is transmitted through the specimen, only reflected excitatory light reaches the objective together with the emitted light and the epifluorescence method therefore gives a high signal-to-noise ratio. The dichroic beam splitter acts as a wavelength specific filter, transmitting fluorescent light through to the eyepiece or detector, but reflecting any remaining excitation light back towards the source.

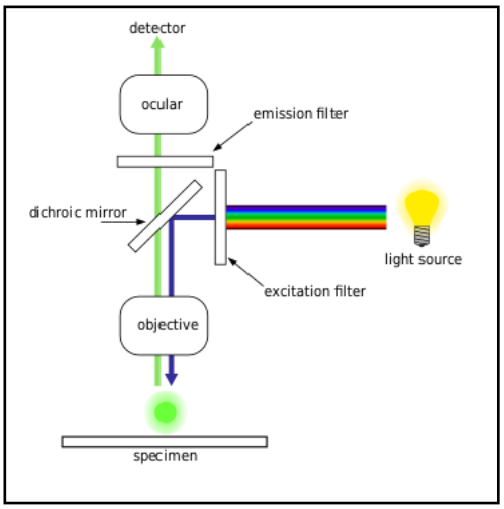

Figure:**fluorescence microscope**

4. AFM

It is a three-dimensional topographic technique with high atomic resolution to measure surface roughness. An AFM needs a micro-scale cantilever with a sharp tip (probe) at its end that is used to scan the specimen's surface. The cantilever is typically silicon or silicon nitride with a tip radius of curvature in the order of nanometres. As the tip reaches the sample surface, the close range attracts a force between the surface and the tip which caused the cantilever to bend towards the surface according to the Hooke's law. The defection of cantilever is called "**Stiffness of cantilever**". The AFM has a Z-scanner that moves the cantilever up and down and XY- scanner moves the sample back and forth underneath the cantilever and the position detector (**Photo diodes**) records the bending of the cantilever. There are two major methods of AFM imaging:-

a. **Contact Mode-** Here the tip is "dragged" across the sample and the boundary of the surface are measured either using the deflection of the cantilever directly or, more commonly using the feedback signal required to keep the cantilever at a constant position. Because the measurement of a static signal is prone to noise and drift, low stiffness cantilevers (low spring constant, k) are used to achieve a large deflections signal while keeping the interaction low. Thus contact mode AFM is almost always done at a depth where overall force is repulsive that is in firm contact with the solid surface.

b. **Non-contact mode-** Here the tip of the cantilever does not contacts the sample surface. The cantilever is instead oscillating at either its resonant frequency or just above where the amplitude of oscillation is typically a few nanometres (1-10 nm). The vanderwaals forces which are the strongest from 1-10nm above the surface tends to decrease the resonance frequency of the cantilever thereby maintaining constant amplitude by adjusting the average tip to sample distance. Measuring this distance allows the scanning software to construct a topological image of the sample surface.

MATERIALS & METHODS

A.

1. **BACTERIAL STRAIN-** Enterotoxigenic *Escherichia coli* 4266 (serogroup 0167; str^R, tet^R, nal^R). The diarrhoea-causing bacteria strain was isolated from the Infectious Disease Hospital (IDH), Kolkata and was characterized by the Department of Bacteriology, National Institute of cholera and Enteric Disease, Kolkata, India.

2. **MICE-** Mice strain Balb/c was purchased from National Centre for laboratory Animal sciences, National Institute of Nutrition, Hyderabad, India. All mices were maintained under specific pathogenic-free conditions in the experimental facility with sterilized food and water.

3. **NUTRIENT BROTH (NB)**-13 gm of nutrient medium was dissolved in 1litre double distilled water followed by sterilization through autoclave. Then it was used as a liquid medium for bacterial cell culture.

4. **AGAR-NB PLATE-** NB media supplemented with 1.5% (w/v) nutrient-agar (NA). NA medium was used as solid medium for bacterial cell culture. Sterilization was done by autoclaving.

5. **STARVATION BUFFER (SB)**- 0.5mM NaCl, 0.17mM KCl, 0.33mM $CaCl_2$, 0.33mM $MgSO_4$, 0.12g Tris and 100µl 1M $CaCl_2$to 100 ml water (pH-8.2).

B.

1.1. Synthesis of Cu@Ag Bimetallic NPs: -

The basic principle for the synthesis of Cu@Ag NPs was the successive reduction of Cu $(NO_3)_2$ and $AgNO_3$ with the use of gelatine and polyvinyl pyrrolidone (PVP) as the capping agents. All the steps of the synthesis process were carried out at 37˚C (ambient conditions) and all the required solutions were prepared in milli-Q water. First, a 7ml solution of 5% (w/v) gelatine was prepared, to which 100µl of 0.2M Cu $(NO_3)_2$ solution was added very slowly and stirred for3-5 mins. NaOH solution (1N) was then added drop-wise, when then added dropwise, till the bluish colour of

gelatine was changed to deep violet colour owing to the formation of Cu- hydroxide complex . The Cu- hydroxide complex was subsequently reduced by dropwise addition of hydrazine hydrate (10 M) and the mixture was allowed to stir for 5 mins. The reduced solution took mild red transparent appearance, indicating complete reduction of the Cu- complex with the formation of metallic copper NPs. To a volume of 1ml of milli-Q water containing 100µl of 0.2M $AgNO_3$ was added very slowly with stirring (addition of Ag ions caused instant change of colour of the solution from mild red to deep red). The stirring was continued for another 5 min and then a 3 ml solution of 300 mg PVP K-30 (SRL, India) was then added and stirred for 3mins, when the Cu@Ag- NPs were finally produced. The NP suspension was stored under ambient conditions. The particles remained stable in suspension for 7-10 days, above which aggregation and precipitation occurred at the bottom of the container.

1.2. Synthesis of Cu@Ag Ionic solution:-

The synthesis of Cu@Ag ionic solution is prepared by mixing $CuNO_3$ and $AgNO_3$ in same proportion as in the preparation of Cu@Ag NPs and the rest is make up by milli-Q water.

2. Characterization of the synthesized Cu@Ag NPs: -

2.1. Absorbance properties of the NPs.

The light absorption property of Cu@Ag NPs suspension was investigated by a spectrophotometer (Shimadzu, UV-1900) in the wavelength region 350-650 nm, using a mixture of gelatine, PVP, NaOH and hydrazine hydrate (in the same proportion as they were used as the ingredients of the NPs preparation) in the reference cuvette.

2.2. Fluorescence properties of the NPs.

The fluorescence property of our nano- composite (diluted 5-10 times in milli-Q water) was investigated by a spectrofluorimeter in Emission wavelength region of 440-700 nm, exciting the sample at 425nm and keeping the slit width fixed at 5nm each.

2.3. Determination of Shape of the NPs: -

The shape of the NPs was measured by Atomic force microscopy (AFM). For investigation, a cover slip ($1cm^2$) for holding the sample was pretreated with Piranha solution (1:3 ratio of 30% H_2O_2/H_2SO_4), then washed subsequently it with deionized water and then dried it keeping it in a 80°C oven for 2-3 hr. About 20µl of the 100

times diluted Cu@Ag NPs suspension was taken on the cleaned and dried cover slip, which was then put in a vacuum desiccators overnight so that a thin film of the NPs was formed over the cover slip. The dried film of NPs was scanned by AFM (Vecco, Innova) in tapping mode, using nanoprobe cantilever made of silicon nitride to obtain 3D image of the particle.

2.4. Determination of hydrodynamic Size& Stability: -

The average hydrodynamic size and stability of the NPs i.e. Zeta Potential was measured by using a DLS instrument (Malvern, Nano- ZS). The cuvette used here is clear disposable Zetasizer for Measurement purpose.

3. Synchronization of bacteria:-

Synchronization of bacteria cells means that all the cells are in the same state of growth cycle. In case of analysis of toxic effects of agents on bacterial cells, it is generally preferred to observe the effects on the healthy synchronized cells. Such grown synchronized cells are so diluted serially that a number of 100-200 cells are individually spread on solid agar plates. A single cell is never visible, but when an agar plate containing cells is allowed to grow overnight at optimum temperature in an incubator, every individual cell, immobilized in the plate, grown to form a visible colony of about 10^5 cells. The number of colonies multiplied by the dilution factor gave the total number of bacteria present in bacterial culture.

3.1. Analysis of antibacterial activity of Cu@Ag NPs

To study the antibacterial property of Cu@Ag NPs the Gram negative ETEC bacteria was selected as the targeted organisms. For this old culture of an ETEC cells was taken out .Then the bacterial culture was thaw-vortexes for at least 30 seconds. Thereafter 100µl of the stock culture was inoculated into 5ml nutrient broth and was kept at 37°Cgyratory Shaker overnight. Cu@Ag bimetallic NPs was prepared and kept undisturbed in dark 24 hrs. Overnight on the same day.

Next day, cells from the overnight culture were diluted 100times (50µl in 5000µl) in NB growth medium and was kept at 37°C in incubator for 2-3 hours to grow the cells at log phase (about 10^8cells/ml) i.e. **synchronizing** of the cells, corresponding to the bacterial optical density 0.2 at 600nm. A set of 16 test tubes were taken on test tube stand and was marked as 0µl, 10µl, 15µl, 20µl, 25µl, 30µl, 35µl, 38µl, 40µl, 85µl, 90µl, 92µl, 94µl, 96µl, 98µl, 100µl, 110µl containing 5ml NB media and is placed inside the LAF along with the Cu@Ag NPs. Cu@Ag ion was prepared just immediately before the experiment starts.

All the test tubes were inoculated with 5µl(0.1%) of ETEC culture. After those test tubes marked 10-40µl& 90-110µl were treated with different concentration of Cu@Ag ionic solution& Cu@Ag NPs solutions respectively as per the test tubes are marked. Then the test tubes were incubated at 37°C gyratory Shaker at 125rpm for 18 hours.

3.2. Determination of MIC& MBC of the NPs

The **MIC** of an antibacterial agent for an particular bacterium is defined as its concentration in the growth medium, by which complete inhibition of bacterial growth occurs without any cell killing after 18 hours of incubation whereas **MBC** of an antimicrobial substance is referred to as concentration which causes 99.99% cell killing of a bacterial population after about 18 hours of incubation. Therefore to determine both MIC & MBC, counting of viable cells (as measured from bacterial colonies on a NA plate) was required according to the following protocol. The grown Synchronized cells that were allowed to incubate in the presence of ascending concentration of the antibacterial agent at 37°C in a gyratory Shaker were taken out and put it inside the LAF. The same volume (100µl) of cell aliquot was withdrawn from each of the incubated cultures followed by dilution in SB properly.

The diluted cell cultures were then spread on NA plates and the plates were allowed to incubate overnight to obtain countable number of colonies. To determine the bacterial titter strength in each set the colony count on the plate was multiplied by corresponding dilution factor.

3.3. Light microscopy study on cell shape & size

The Cu@Ag NPs mediated changes in the cell shape and size were examined by fluorescence microscopy in the phase contrast mode. An aliquot of 10µl from each of the 18 hours incubated cultures (different concentration of Cu@Ag NPs) was taken on a clean and grease free slide covered with a coverslip on which a drop of immersion oil was given and then viewed through 100X objective.

The average shape and size of the cells were determined by viewing cells at different fields.

4. In vivo analysis of the effect of NPs on ETEC-Balb/C Mice model

Male Balb/C mice (weight should be 25gm or above otherwise the mice will die after infection immediately) were obtained from National Centre for laboratory Animal sciences, National Institute of Nutrition, Hyderabad, India. The mice were housed in clean polystyrene cages with stainless steel wire and provided with food and water ad libitum. The mice were acclimated into a new environment before being used for experimental purposes.

For the in vivo analysis of the effect of NPs and subsequent ions after infected with ETEC onto Balb/C Mice model the 4 male mices were divided into 4 groups: A, B, C

and a Control group. The weight of each mouse was noted before the infection. After this group A, B,C mice were treated with 5×10^8 cells of ETEC intraperitoneally, by means of hypodermic needle & the control was remain untreated.
After 3 hours of infection, observations were made and group B & C were treated with 6.27µg/ml of NPs and ionic solution respectively intragastrically, by means of esophageal catheter and group A is left as infected (Dose I). Dose II & Dose III was given to the mice after 6 & 12 hrs of Dose I with same amount of NPs and ionic solution.

4.1. DISEASE ACTIVITY INDEX (DAI) Score: -

The DAI score of an Organism is defined as the average of the sum of Weight loss score Stool viscosity score and haematochezia score.

$$\mathbf{DAI} = \frac{\boldsymbol{weight\ loss\ sccore + Stool\ viscosity\ score + haematochezia\ score}}{\mathbf{3}}$$

4.2. Standard Table for DAI Score: -

SCORE	0	1	2	3	4
Loss of Weight	Normal faeces	1-5%	5-10%	10-20%	>20%
Stool Consistency	Normal	loose stool	Watery diarrhoea	Slimy diarrhoea	Severe Watery diarrhoea
Occult blood in faeces	Negative			Positive	Bloody stools

Normal faeces: granular stool; loose stool: mushy stool that did not stick to the anus; diarrhoea: watery stool that stuck around the anus.

The weight of the body, faecal characteristics and activity of each mouse was observed upto 8days and using these days the DAI score was calculated and recorded on an observation table. Note that the mice should we given adequate food and water regularly and should be kept in a sterile environment with suitable temperature and pressure ad libitum so as to keep them healthy.

RESULTS AND DISCUSSION

1.1. Synthesis of Cu@Ag NPs: -

During the synthesis of bimetallic Cu-Ag NPs, successive reduction of copper and silver was expected to synthesize NPs of core-shell structure (shell of Ag^0 atoms on a core of Cu^0 atoms). According to the report hydrazine mediated reduction of copper salt in presence of gelatine caused gradual nucleation of Cu^0 atoms within the gelatine, producing gelatine stabilized Cu^0 NPs. However, after addition of $AgNO_3$ caused instant change in the colour of solution from mild red to deep red which means deposition of Ag^0 atoms on the nucleated core of Cu^0; subsequently addition of PVP makes this bimetallic NPs stable by forming an outer PVP layer.

The deposition of Ag^0 atoms was probably due to the reduction of Ag^{+1} ion to Ag^0 with simultaneous oxidation of Cu^0 atoms at the periphery of the Cu^0 core. Otherwise, if Ag^{1+} is reduced by hydrazine there would be trace of Ag^0 NPs also beside Cu@Ag NPs; however optical properties (discussed later) gives evidence that there is no Ag NPs in our NP suspension. Therefore, the synthesized NPs contain only Core of Cu^0 atoms which are surrounded by Ag^0 atoms.

1.2. CHARACTERISTICS FEATURES OF Cu@Ag NPs: -

❖ ABSORBANCE PROPERTIES: -

Bimetallic NPs can take one of the two architectural forms either random organization of the two compositing metals leads to formation of alloy-NPs or an upcoming metal gets deposited on a core assembly of other metal leading to the formation of core-shell NPs. UV-Vis spectroscopy is a good technique to confirm the architectural form of any bi-metallic NPs which arises from its localized Surface-Plasmon-Resonance (SPR) (**Banik et al., 2014A; Valodkar et al., 2011**). Bimetallic random alloy-NPs are identified by single SPR peak wavelengths of individual NPs of the two metals (**Rahman et al.., Kiani et al.., Valodkar et al.., 2011**). In case of core shell structures, two SPR peaks at wavelengths of the individual metal NPs are generally found (Chao Zhang et al., 2015; Zhang et al., 2009) although in some cases a single peak is observed, keeping the other peak indistinguishable (**Petrovic et al., 2015**).In reality if the corresponding metals are mixed in varying ratios during NPs synthesis. With increasing mass percentage of one metal, if the peak shifts gradually towards red zone of the spectrum or vice versa, the bimetallic nanoparticles must be random alloy in nature (**Rahman et al., 2012; Kiani et al., 2011**). In that a linear relationship is maintained between the SPR peak and the increasing mass percentage of a metal of the two (**Rahman et al., 2011**). However, in case of core shell pattern, there is no variation of the composition ratio of compositing metals.

The light absorption property of Cu@Ag NP suspension was investigated by a spectrophotometer (Shimadzu UV-1800) in the wavelength 350-650 nm. The reason behind selecting this wavelength region was that the SPR peak range of AgNP and CuNP suspension separately was found to be (370-410) nm and (540-600) nm respectively (**Banik et al., 2014A; Rahman et al.,2012; Kiani et al., 2012**). Freshly prepared NP suspension was diluted 5 times in milli-Q water and its absorbance was monitored using a mixture of gelatine, PVP, NaOH and hydrazine hydrate (in the same proportion as they were present in the Cu@Ag suspension prepared at a molar ratio 1:1 of the metals, depicted that it had a single SPR peak at 430nm (1.6 O.D) which lied between the SPR peak range of AgNP (370-410nm) and CuNP (540-600nm); however, more closed to the AgNP peak. This result implied that the NP, prepared by our method was randomly organized NA.

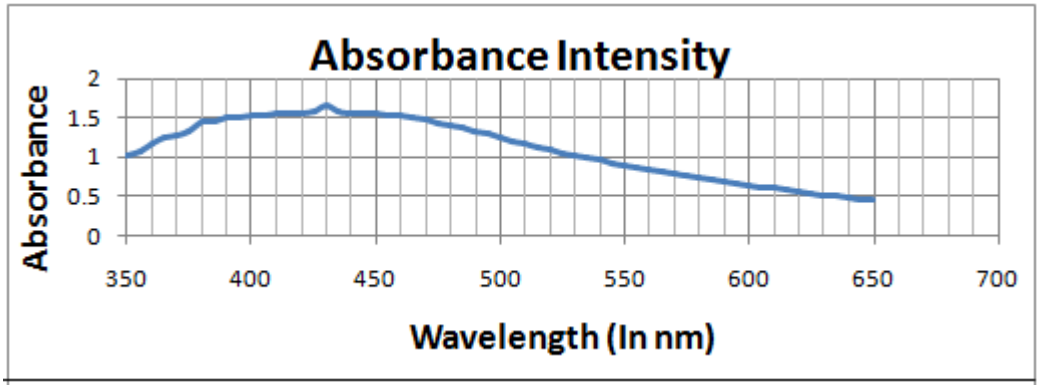

However, our successive reduction method of synthesis was expected to produce Cu@Ag of core shell architecture. This paradox was cleared by preparing the NPs at different composition ratios of Cu and Ag (Cu:Ag) = 0.5:1, 1:1, 1.5:1, 2:1, 2.5:1, 3:1 and

the UV-Vis spectrophotometric study of the NPs was performed (**Banik et al; 2014A**). The spectra demonstrated that above the ratio of 1:1, a second SPR peak, in addition to the peak at 425nm appeared at 525nm (close to the SPR peak wavelength of CuNP); these Plasmon peak didn't shift in wavelength but their intensity increased with the increase in the Cu-concentration. This result depict the formation of core shell structure of Cu@Ag NPs which shows a single SPR peak at a wavelength close to the SPR peak range of shell metal.

❖ FLUORESCENCE PROPERTIES: -

AgNP and CuNP were reported to have individual fluorescence property with emission at 485 and 645 nm respectively, when they were excited at their Plasmon maxima (**Valodkar et al., 2011**). In case of AgNP, excitation of d-band electrons to sp-band was responsible for origin of fluorescence, whereas for CuNP electronic transitions from excited states to d-orbital were responsible for fluorescence (**Rahman et al., 2012; Valodkar et al., 2011**). Bimetallic Cu@Ag suspension was also reported to have fluorescence property (**Rahman et al., 2012**).

The fluorescence of our nanoparticle (diluted 5 times in milli-Q water) was investigated by a spectrofluorimeter in the emission wavelength region 440-700nm, exciting the sample at its SPR peak 425nm with slit width fixed at 5nm. There was a single emission peak at (495nm) very close to the fluorescence peak of AgNPs.

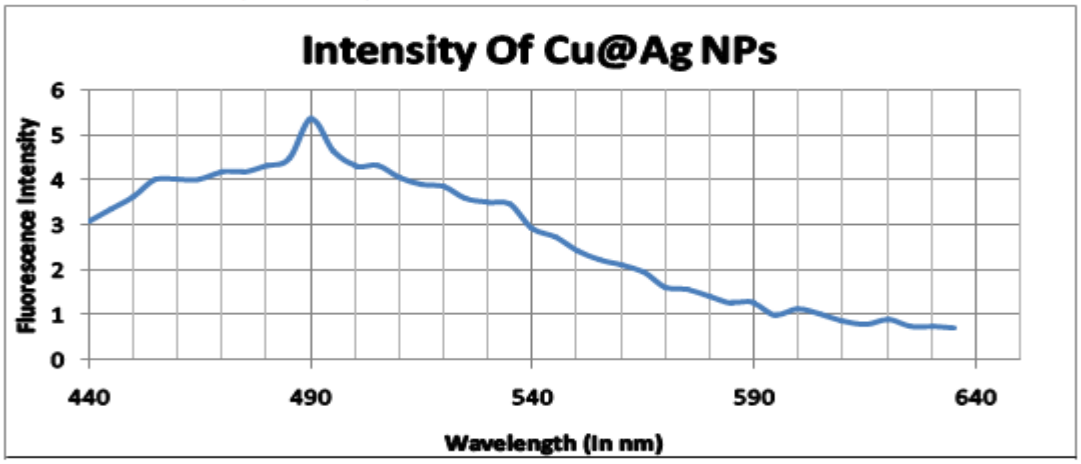

Moreover, excitation of the NP suspension at the Plasmon peak of CuNPs (570 nm) showed no considerable fluorescence. These results depict that CuNPs were embedded within AgNPs forming a core-shell structure. In such structure excitation of Cu@AgNPs at 425 nm showed the fluorescence from AgNPs; however, excitation at 570nm might not show fluorescence possibly due to inaccessibility of the CuNPs to be excited.

❖ Determination of Shape, Zeta potential and Size:-

The average hydrodynamic size of the Cu@Ag NPs as determined by DLS was 76.26nm in diameter which signifies the size of the NPs is in well-defined Nano range to be used for challenging the bacterial permeability (S.A $\alpha\frac{1}{r}$) more efficiently and the PDI value comes out to be 0.289 which signifies that the sample is slightly polydispersive i.e. containing few numbers of heterozygous molecular size molecule. The stability of any NP is generally signified by its Zeta potential. In suspension, association of the charge groups on any NP surface with the opposite charge groups of the solvents results in a

potential difference around surface of the NP, is known as Zeta Potential. The higher absolute value of the Zeta potential (either +ve or-ve) imparts higher stability of the NP. Here the Zeta Potential of the NP comes out to be -15.5mV which defines that theNPs present in the sample were moderately stable and well-dispersed in the suspension up to 5-7 days above which a tiny visible reddish precipitate was observed after about two weeks, due to slow oxidation followed by aggregation.

Moreover AFM studies on the NPs reveals that the size of the particle was found out to be 78 nm and is spherical in shape.

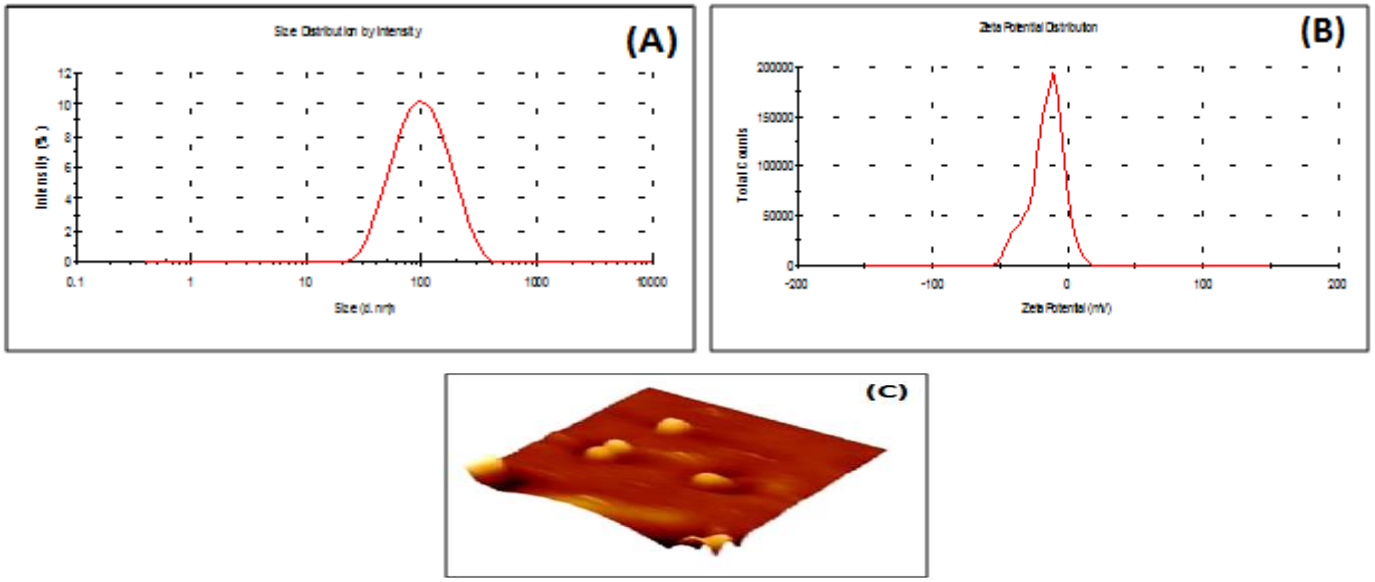

Figure: (A) Size distribution by Intensity of Cu@Ag NPs. (B) Zeta potential distribution of Cu@Ag NPs.

(C) 3D AFM images of Cu@Ag NPs.

1.3. Antibacterial properties (MIC & MBC) :-

Initial number of ETEC cells before incubation = 2×10^7 cells.

Table for Cu@Ag NP treatment-(1)

Total Amount of Cu@AgNPs (µg/ml)	Amount of AgNP (µg/ml) [17.975]	Amount of CuNP (µg/ml) [10.58]	Total number of viable cells (Plate count)
0	-	-	2.5×10^9
5.1399	3.2355	1.9044	5.2×10^8
5.254	3.3074	1.94672	4.0×10^8
5.368	3.3793	1.98904	1.9×10^8
5.483 (MIC)	3.4512	2.03136	3.0×10^7
5.597	3.5231	2.07368	8.2×10^6
5.711	3.595	2.116	3.4×10^6
6.27 (MBC)	3.9545	2.3276	1.4×10^4

Table for Cu- Ag Ion Treatment-(2)

Total Amount of	Amt. of Ag^{2+} ion	Amt. of Cu^{2+} ion	Total number of

Cu^{2+}, Ag^{2+} ions (µg/ml)	(µg/ml) [17.975]	(µg/ml) [10.58]	viable cells (Plate count)
0	-	-	2.5×10^9
1.428	0.899	0.529	5.8×10^8
1.714 (MIC)	1.079	0.635	2.2×10^7
1.999	1.258	0.741	1.08×10^6
2.17 (MBC)	1.366	0.804	2.0×10^4
2.284	1.438	0.847	4.0×10^2

The tables1 & 2 depicted in the previous page shows the amount of Cu@Ag NPs and Cu^{2+} , Ag^{2+} ions needed to inhibit the bacterial growth without any killing (MIC) and to kill 99.9% cell killing of a bacterial population (MBC) after 18 hours of incubation.
Here the Minimum Inhibitory concentration (MIC) and Minimum Bacterial concentration (MBC) of Cu@Ag NPs are 5.483 µg/ml and 6.27 µg/ml respectively.
Also the Minimum Inhibitory concentration (MIC) and Minimum Bacterial concentration (MBC) ofCu^{2+}, Ag^{2+} ions are 1.714µg/ml and 2.17 µg/ml respectively.
This result also provides us the information that the concentration of Nanoparticle required to act as MIC & MBC on ETEC is more than the concentration of Cu^{2+}, Ag^{2+} ions. Hence Ions particles are more effective than nanoparticles at lower concentrations but with the increase in incubation time the effectiveness of ions particles on bacterial culture ceases and the growth of bacteria became visible.

1.4. Light microscopic Study on Cell Shape & Size :-

Filamentation is known to be a primary defense mechanism for the cells under the environmental threats of consumption and killing; cell growth continues in the absence of cell division and results in the formation of elongated organisms that have multiple copies. The light microscopy study of Cu@Ag NPs mediated changes in ETEC cells shows that there is no occurrence of cell filamentation due to inhibition of cell division rather the cells becomes circular in shape compared to normal cells that are of rod shape and gets clumped onto each other. Moreover there is no uniform distribution of cell number in different fields of view. In all, cell filamentation is not the type of cell damage repair mechanism incurred by bacteria due to inhibition of cell division.

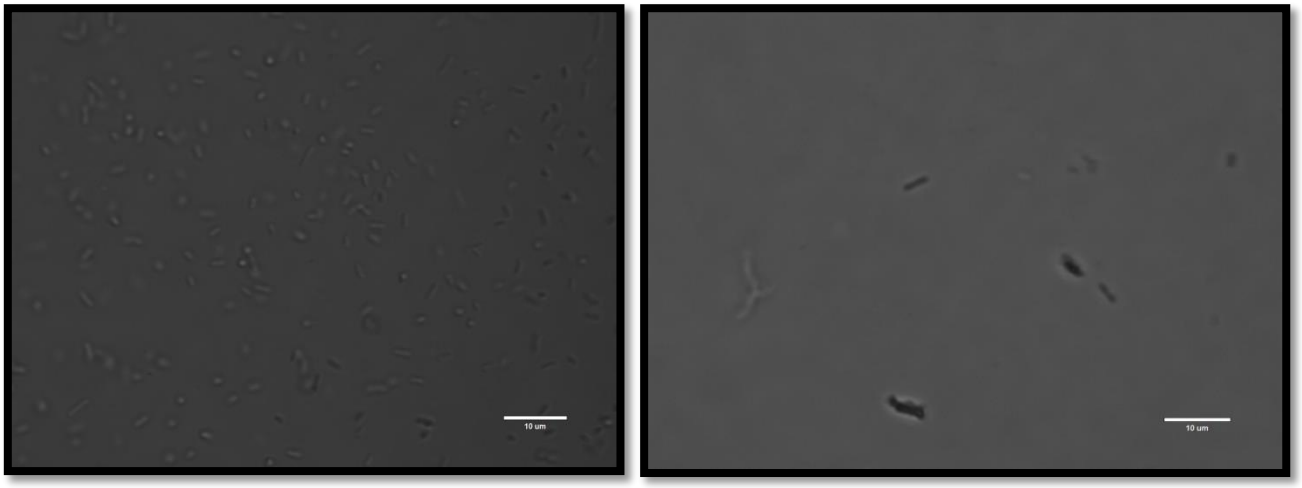

Figure: - Microscopic view of **(A)** untreated cells [Control]. **(B)** Cu@Ag NPs treated cells.

1.5. In vivo analysis of the effect of NPs and subsequent ions after infected with ETEC onto Balb/C Mice model:-

After the successful infection of ETEC cells onto Balb/C mice, observations were made after the treatment with NPs and ion treatment for around 8 days. The following table represents the observations made from day0 to day7.

	BODY WEIGHT LOSS				STOOL CONSISTENCY			
	Control	Infected	NP treated	Ion treated	Control	Infected	NP treated	Ion treated
Day0	0% Score- 0	3.4% Score- 1	0% Score- 0	0% Score- 0	Normal Score- 0	Waterydiarrhea Score- 2	Normal Score- 0	Normal Score- 0
Day1	0% Score- 0	6.19% Score- 2	15% Score- 3	7.18% Score- 2	Normal Score- 0	Slimy diarrhea Score- 3	Normal Score- 0	Loose Stool Score- 1
Day2	0% Score- 0	-	19.6% Score- 3	15.7% Score- 3	Normal Score- 0	-	Loose Stool Score- 1	Waterydiarrhea Score- 2
Day3	0% Score- 0	-	16.8% Score- 3	-	Normal Score- 0	-	Loose Stool Score- 1	-
Day4	0% Score- 0	-	11.7% Score- 3	-	Normal Score- 0	-	Normal Score- 0	-
Day5	0% Score- 0	-	11.5% Score- 3	-	Normal Score- 0	-	Normal Score- 0	-
Day6	0% Score- 0	-	9% Score-2	-	Normal Score- 0	-	Normal Score- 0	-
Day7	0% Score- 0	-	5% Score- 1	-	Normal Score- 0	-	Normal Score- 0	-

The above table illustrates the body weight loss and stool consistency of the mice in four different condition: Uninfected, Infected (only), Infected & NP treated, and Infected & Ion treated. Before the experiment, no significant difference in body weight between different groups and the stool were granular. In ***uninfected*** mice there is no significant change in body weight and stool. After the administration of ETEC the mice appeared depressed, started shivering continuously and reduced food and water uptake; thus losing weight with loose both in case of ***Infected mice (only)*** and ***infected & Cu^{2+},Ag^{2+}ion*** mice. Moreover the DAI score(average) of the infected mice was 2 in both cases and after that the mice dies due to infection in the first case and due to ionic effect of Cu^{2+} Ag^{2+} in the second case respectively.

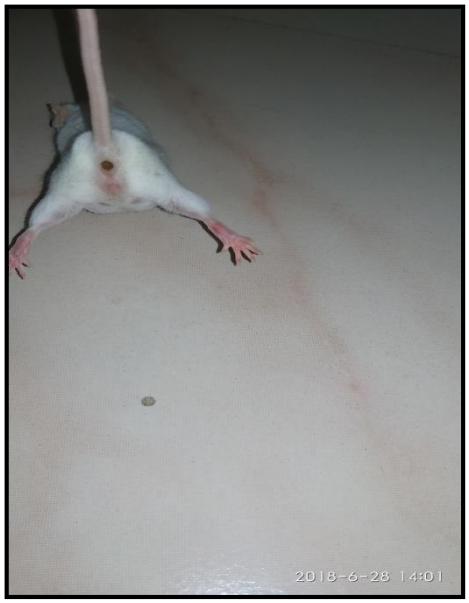

Figure: - **(A)** Cu@Ag NPs treated mice producing Normal stool after infection

(B) Infected mice producing Loose stool.

In ***Infected & Cu@Ag NPs*** treated condition the mice started shivering after the infection but later after the NP treatment the mice gets relaxed as the dosage number increases; loose stool and weight loss were observed till day2 and the DAI was 2. After 3rd day, the DAI scores declines and the mice survives.

INFERENCE

In this communication we studied a new method of synthesis for Cu@Ag NPs with $CuNO_3$ and $AgNO_3$ as the substrates and gelatine and PVP as the stabilizers and remained highly stable for a month in response to Zeta potential of the NPs.

In this process, more than 90% of the $CuNO_3$ and $AgNO_3$ were reduced to Cu@Ag NPs. Moreover from the DLS AFM studies, the average size of the NPs was found out to be in the range of 70-80 nm. Moreover it appeared from the AFM images that the Nanoparticles were spherical in shape and coated by gelatine and PVP at the core and shell respectively. Hence this protective layer probably inhibits the rapid oxidation of the metals contributing to the increased stability of our NPs.

During the antibacterial activity study of our synthesized Nanoparticles we concluded that the MIC & MBC were 5.483 and 6.27 µg/ml respectively compared to the Ion particles whose MIC & MBC were1.714 and 2.17 µg/ml respectively. This result concludes that the ions are more effective at lower concentration than the nanoparticles. The fact that filamentation is not the key antibacterial property for the ETEC cells was confirmed through fluorescence microscopy where we observe that there was no elongation of cells as the type of cell damage repair system rather the cells becomes circular and gets clumped onto a dead cell mass.

During the in vivo analysis in higher mammals like Balb/C Mice model to make this Cu@Ag NPs functional to combat deadly pathogenic multiple antibiotics-resistance bacteria, challenging the major cause of death in tropical countries. The results of our ongoing study on survivability of ETEC injected mice by Cu@Ag NPs and Cu^{2+}, Ag^{2+} ions, administered through oral dose shows that although ion are more effective at lower concentration compared to the nanoparticle but the mice dies due to ionic toxic effects, whereas the nanoparticle treated mice survives and shows its advantageous over the ions.

Finally it could be inferred that the diarrheal diseases caused by the principal bacterial genii as the major health problem in developing countries could be eliminated using the Cu@Ag NPs treatment. This is one such method that would provide a hope for the people who have got infected. There are many other methods to resist diarrheal diseases but it is one of the simplest rescue technique for them.

REFERENCES

1. Milon Banik, Mousumi Patra, Debanjan Dutta, Riya Mukherjee and Tarakdas Basu 2018 simple robust method of synthesis of copper–silver core–shell nano-particle: evaluation of its structural and chemical properties with anticancer potency **29** 325102.
2. Chatterjee A K, Chakraborty R and Basu T 2014 Mechanism of antibacterial activity of copper nanoparticles Nanotechnology **25** 135101.
3. Riya Mukherjee, Mousami Patra, Dbanjan Dutta, Milon Banik, Tarakdas Basu 2016 Tetracyclin-loaded calcium phosphate : Rejuvenation of an absolute antibiotic to further action.
4. Wagner V, Dullaart A, Bock A-K and Zweck A 2006 The emerging nano medicine landscape Nat. Biotechnol. **24** 1211–7.
5. Chatterjee A K, Chakraborty R and Basu T 2014 Mechanism of antibacterial activity of copper nanoparticles Nanotechnology **25** 135101.
6. Valodkar M, Modi S, Pal A and Thakore S 2011 Synthesis and anti-bacterial activity of Cu, Ag and Cu–Ag alloy nanoparticles: a green approach Mater. Res. Bull**. 46** 389-9.
7. Ruparelia J P, Chatterjee A K, Duttagupta S P and Mukherji S 2008 Strain specificity in antimicrobial activity of silver andcopper nanoparticles Acta Biomater **4** 707-16.
8. Prabhu S and Poulose E K 2012 Silver nanoparticles: mechanism of antimicrobial action, synthesis, medical applications, and toxicity effects Int. Nano Lett **2** 32.
9. Lok C, Ho C, Chen R, He Q, Yu W, Sun H, Tam P K, Chiu J and Che C 2006 Proteomic analysis of the mode of antibacterial action of silver nanoparticles research articles J. Proteome Res. **5** 916-24.
10. Sankar R, Karthik A, Prabu A, Karthik S, Shivashangari K S and Ravikumar V 2013 Origanum vulgare mediated biosynthesis of silver nanoparticles for its antibacterial and anticancer activity Colloids Surf. B **108** 80-4.
11. Petrović S, Salatić B, Milovanović D, Lazović V, Živković L, Trtica M and Jelenković B 2015 Agglomeration in core–shell structure of CuAg nanoparticles synthesized by the laser
ablation of Cu target in aqueous solutions J. Opt. **17** 25402.
12. Rahman L U, Qureshi R, Yasinzai M M and Shah A 2012 Synthesis and spectroscopic characterization of Ag–Cu alloynanoparticles prepared in various ratios C. R. Chim. **15** 533-8.
13. Wang H K, Yi C Y, Tian L, Wang W J, Fang J, Zhao J H and Shen W G 2012 Ag–Cu bimetallic nanoparticles prepared by microemulsion method as catalyst for epoxidation of styrene J. Nanomater.**8** 453915
14. Kiani Z 2012 Low temperature formation of silver and silver–copper alloy nano-particles using plasma enhanced 21 Nanotechnology 29 (2018) 325102 M Banik et al
hydrogenation and their optical properties World J. Nano Sci. Eng. **2** 142–7
15. Banik M and Basu T 2014 Calcium phosphate nanoparticles: a study of their synthesis, characterization and mode of interaction with salmon testis DNA Dalton Trans. **43** 3244–59
16. Zhang J, Liu H, Wang Z and Ming N 2007 Preparation and optical properties of silica@Ag–Cu alloy alloy core–shell composite colloids J. Solid State Chem. **180** 1291–7
17. Shankar S S, Rai A, Ahmad A and Sastry M 2004 Rapid synthesis of Au, Ag, and bimetallic Au core–Ag shell nanoparticles using Neem (Azadirachta indica) leaf broth
J. Colloid Interface Sci. **275** 496–502
18. Chatterjee A K, Sarkar R K, Chattopadhyay A P, Aich P, Chakraborty R and Basu T 2012 A simple robust method for synthesis of metallic copper nanoparticles of high antibacterial potency against E. coli Nanotechnology **23** 85103
19. Chakraborty R, Sarkar R K, Chatterjee A K, Manju U, Chattopadhyay A P and Basu T 2015 A simple, fast and cost-effective method of synthesis of cupric oxide nanoparticle with promising antibacterial potency: unraveling the biological and chemical modes of action Biochim. Biophys. Acta, Gen. Subj. **1850** 845–56

20. Peng H, Qi W, Li S and Ji W 2015 Modeling the phase stability of Janus, core–shell, and alloyed Ag–Cu and Ag– Au nanoparticles J. Phys. Chem. C **119** 2186–95
21. Dutta D, Mukherjee R, Patra M, Banik M, Dasgupta R, Mukherjee M and Basu T 2016 Green synthesized cerium oxide nanoparticle: a prospective drug against oxidative
harm Colloids Surf. B **147** 45–53
22. Chakraborty R, Sarkar R K, Chatterjee A K, Manju U,Chattopadhyay A P and Basu T 2015 A simple, fast andcost-effective method of synthesis of cupric oxide nanoparticle with promising antibacterial potency: unraveling the biological and chemical modes of action Biochim. Biophys. Acta, Gen. Subj. **1850** 845–56
23. Agnihotri S, Mukherji S and Mukherji S 2014 Size-controlled silver nanoparticles synthesized over the range 5–100 nm using the same protocol and their antibacterial efficacy RSC Adv. **4** 3974–83
24. Laha D, Bhattacharya D, Pramanik A, Santra C R, Pramanik P and Karmakar P 2012 Evaluation of copper iodide and copper phosphate nanoparticles for their potential cytotoxic effect Toxicology Res**. 1** 131
25. Garcia-Gutierrez D I, Gutierrez-Wing C E, Giovanetti L, Ramallo-López J M, Requejo F G and Jose-Yacaman M 2005 Temperature effect on the synthesis of Au–Pt bimetallic nanoparticles J. Phys. Chem. B **109** 3813–21
26. Murphy A, Sheehy K, Casey A and Chambers G 2015 Potential of biofluid components to modify silver nanoparticle toxicity J. Appl. Toxicology **35** 665–80
27. Green wood, R, Kendall K (1999). "Electroacoustic studies of moderately concentrated colloidal suspension". Journal of the European Ceramic Society. 19(4): 479-488
28. Hanaor , D.A.H; Michelazzi , M; Leonelli , C; Sorrell , C.C (2012). "The effects of carboxylic acids on the aqueous dispersion and electrophoretic deposition of ZnO_2" of the European Ceramic Society. 32(1): 235-44
29. Zhang Y, Yang M, Portney N G, Cui D, Budak G, Ozbay E, Ozkan M and Ozkan C S 2008 Zeta potential: a surface electrical characteristic to probe the interaction of nanoparticles with normal and cancer human breastepithelial cells Biomed. Microdevices 10 321–8
30. Biryukova M I, Yurkov G Y, Syrbu S A and Taratanov N A 2014 Synthesis and structure of copper nanoparticles and their antiinfection properties Inorg. Mater.: Appl. Res. **5** 54–60
31. Abdul Salam A, Singaravelan R, Vasanthi P and Bangarusudarsan Alwar S 2015 Electrochemical fabrication of Ag–Cu nano alloy and its characterization: an investigation J. Nanostruct. Chem. **5** 383–92
32. Sharma S, Ahmad N, Prakash A, Singh V N, Ghosh A K and Mehta B R 2010 Synthesis of crystalline Ag nanoparticles (AgNPs) from microorganisms Mater. Sci. Appl. **1** 1–7
33. Langlois C, Li Z L, Yuan J, Alloyeau D, Nelayah J, Bochicchio D, Ferrando R and Ricolleau C 2012 Transition from core–shell to Janus chemical configuration for bimetallic nanoparticles Nanoscale **4** 3381
34. Chen D-H and Chen C-J 2002 Formation and characterization of Au–Ag bimetallic nanoparticles in water-in-oil microemulsions J. Mater. Chem. **12** 1557–62
35. Basu S and Chakravorty D 2006 Optical properties of nanocomposites with iron core iron oxide shell structure J. Non-Cryst. Solids **352** 380–5
36. R.L. Guerrant , M.Kosek, S.Moore, B. Lorntz, R. Brantley, A.A.Lima, Magnitude and impact of diarrheal dsease, Arch.Med.Res. 33(2002) 351-355
37. M. Kosek, C. Bern, R.L. Guerrant, The global burden of diarrhoeal disease, as estimated from studies published between 1992 and 2000, Bull. World Health Organ. 81 (2003) 197–204.
38. G.B. Nair, T. Ramamurthy, M.K. Bhattacharya, T. Krishnan, S. Ganguly, D.R. Saha, K. Rajendran, B. Manna, M. Ghosh, K. Okamoto, Y. Takeda, Emerging trends in the etiology of

enteric pathogens as evidenced from an active surveillance of hospitalized diarrhoeal patients in Kolkata, India, Gut. Pathog. 2 (2010) 4.
39. F. Qadri, A.M. Svennerholm, A.S. Faruque, R.B. Sack, Enterotoxigenic Escherichia coli in developing countries: epidemiology, microbiology, clinical features, treatment, and prevention, Clin. Microbiol. Rev. 18 (2005) 465–483.
40. P. Gao, X. Nie, M. Zou, Y. Shi, G. Cheng, Recent advances in materials for extendedrelease antibiotic delivery system, J. Antibiot. 64 (2011) 625–634.
41. M.N. Seleem, P. Munusamy, A. Ranjan, H. Alqublan, G. Pickrell, N. Sriranganathan, Silica-antibiotic hybrid nanoparticles for targeting intracellular pathogens, Antimicrob. Agents Chemother. 53 (2009) 4270–4274.
42. E. Lu, S. Franzblau, H. Onyuksel, C. Popescu, Preparation of aminoglycoside-loaded chitosan nanoparticles using dextran sulphate as a counterion, J. Microencapsul. 26 (2009) 346–354.
43. W.S. Cheow, M.W. Chang, K. Hadinoto, Antibacterial efficacy of inhalable levofloxacin-loaded polymeric nanoparticles against E. coli biofilm cells: the effect of antibiotic release profile, Pharm. Res. 27 (2010) (1597-09).
44. B. Epe, P. Woolley, H. Hornung, Competition between tetracycline and tRNA at both P and A sites of the ribosome of Escherichia coli, FEBS Lett. 213 (1987) 443–447.
45. D.E. Brodersen, W.M. Clemons (Jr.), A.P. Carter, R.J. MorganWarren, B.T. Wimberly, V. Ramakrishnan, The structural basis for the action of the antibiotics tetracycline, pactamycin, and hygromycin B on the 30S ribosomal subunit, Cell 103 (2000) 1143–1154.
46. I. Chopra, M. Roberts, Tetracycline antibiotics: mode of action, applications, molecular biology, and epidemiology of bacterial resistance, Microbiol. Mol. Biol. Rev. 65 (2001) 232–260.
47. B.S. Speer, N.B. Shoemaker, A.A. Salyers, Bacterial resistance to tetracycline: mechanisms, transfer, and clinical significance, Clin. Microbiol. Rev. 5 (1992) 387–399.
48. S.R. Connell, D.M. Tracz, K.H. Nierhaus, D.E. Taylor, Ribosomal protection proteins and their mechanism of tetracycline resistance, Antimicrob. Agents Chemother. 47 (2003) 3675–3681.
49. Justice S S, Hunstad D A, Cegelski L and Hultgren S J 2008 Morphological plasticity as a bacterial survival strategy Nature. Rev. Microbiol. 6 162-8
50. Du W L, Xu Z R and Fan C L 2008 Preperation, characterization and antibacterial properties against E.coli k_{88} of chitosan nanoparticle loaded copper ions Nanotechnology. 19 1-5